REPORT

METALLURGY

Constrained minimal-interface structures in polycrystalline copper with extremely fine grains

X. Y. Li[1]*, Z. H. Jin[1,2], X. Zhou[1], K. Lu[1]*

Metals usually exist in the form of polycrystalline solids, which are thermodynamically unstable because of the presence of disordered grain boundaries. Grain boundaries tend to be eliminated through coarsening when heated or by transforming into metastable amorphous states when the grains are small enough. Through experiments and molecular dynamics simulations, we discovered a different type of metastable state for extremely fine-grained polycrystalline pure copper. After we reduced grain sizes to a few nanometers with straining, the grain boundaries in the polycrystals evolved into three-dimensional minimal-interface structures constrained by twin boundary networks. This polycrystalline structure that underlies what we call a Schwarz crystal is stable against grain coarsening, even when close to the equilibrium melting point. The polycrystalline samples also exhibit a strength in the vicinity of the theoretical value.

The end-member structures for solids are single crystals, where atoms are arranged in ordered crystal lattices throughout the sample, and amorphous solids or glasses, where atomic arrangements are disordered with short- or medium-range ordering only (*1*). Metals usually exist in the form of polycrystalline solids, which are between these two extremes. They are made up of smaller crystallites (called grains) that are separated by a variety of boundaries where atomic arrangements are normally disordered. The disordered grain boundary (GB) is what makes polycrystalline metals thermodynamically unstable.

Polycrystalline materials tend to become more stable when GBs are eliminated, until they ultimately become single crystals. An example of this process is how the grains in polycrystals may coarsen through GB migration that usually occurs at temperatures below half of the melting point (*2*). The coarsening temperature drops with decreasing grain size, going as far down as room temperature in some nanograined metals (*3*). For fine-grained polycrystals with a high enough GB density, transforming into a metastable amorphous state is an alternative option to stabilization. This state is anticipated from a thermodynamic point of view, and amorphization has been observed in a number of metallic alloys [e.g., Ni-P (*4*) and Ni-W (*5*)] as grain sizes were reduced below certain limits (typically a few nanometers). However, under the thermodynamic and kinetic constraints, amorphous states are compositionally selective and rarely form for most metallic alloys and pure metals under conventional conditions. A fundamental question to be answered is whether other metastable structures may be adopted when polycrystalline grains are steadily refined to extremely small scales.

We have recently found that when grains of pure Cu and Ni are refined to a few tens of nanometers in size through plastic deformation, the autonomous GB relaxation into low-energy states is triggered with GB dissociations (*6*). The corresponding GB energy decreases accordingly, which leads to a substantial elevation in the thermal and mechanical stabilities of nanograins against coarsening at smaller sizes (*6*, *7*). This observation suggests the possibility that nanograined structures may evolve into more-stable states by approaching the grain-size extreme. We discovered, through experimental and molecular dynamics (MD) simulations, a metastable state in polycrystalline pure Cu with grain sizes of a few nanometers. The state is formed by the evolution of GBs into three-dimensional (3D) minimal-interface structures constrained by twin boundary networks. In this type of polycrystal, grain coarsening is effectively suppressed, even close to the melting point. The strength is also close to the theoretical value of Cu.

With a two-step plastic deformation process of surface mechanical grinding treatment followed by high-pressure torsion in liquid nitrogen, grains of polycrystalline Cu with a purity of 99.97 wt % were refined into the nanometer scale (see the supplementary materials). Bright-field transmission electron microscopy (TEM) images of the extremely fine grains in the as-prepared specimens showed a typical manifold structure (Fig. 1A), as is normally observed in the bicontinuous lipid-water phases (*8*). The specimen consisted of irregularly shaped aggregates or chains connected to each other that form continuous networks. By increasing the magnification, we observed that the aggregates are made up of several individual grains of a few nanometers in size. Among grains of similar contrast in an aggregate, we detected either twin relationships or coincidence site lattice (CSL) boundaries. For example, as indicated by the fast Fourier transform (FFT) patterns of an aggregate consisting of five grains (Fig. 1B), we observed two sets of Σ3 boundaries on $(1\bar{1}1)$ and $(\bar{1}\bar{1}1)$ planes, respectively, and a CSL boundary with a misorientation of 21° between G4 and G5.

TEM images obtained in high-resolution mode of the ultrathin foil specimens showed nanosized crystallites with various orientations in the as-prepared Cu (Fig. 1C). Grains were roughly equiaxed with a uniform size distribution, with most grains <10 nm in size. Selected area electron diffraction covering a large number of grains showed nearly continuous diffraction rings of face-centered cubic (fcc) Cu, an indication of seemingly random orientations of the polycrystallites. The tiny crystallites are connected with each other by atomically distinct boundaries. We did not detect amorphous phases or pores. The full crystallinity of the as-prepared Cu sample is in concert with x-ray diffraction patterns, where sharp diffraction peaks show up without a diffused amorphous peak.

Our procession electron diffraction measurements under TEM (Fig. 1D) revealed that a considerable fraction of GBs (~25%) are Σ3 twin boundaries with a misorientation of 60° in the sample. Other interfaces separating grains have randomly distributed misorientations, among which different types of low-Σ CSL boundaries were detected as well, constituting ~20%. This is in agreement with our other observations (Fig. 1, A and B). As in the magnified images (Fig. 1E), some boundaries are associated with GB structural units as previously observed, underlying the typical structures of relaxed GBs. All of these structural characteristics support the assumption that the GBs are in relaxed states, which is consistent with the decreased GB energy in the relaxed nanograined Cu below the critical grain size (*6*).

We characterized individual grains by properly tilting the specimens under high-resolution TEM so as to resolve their lattice images. We identified diverse geometries for plenty of individual grains. Rather than curved boundaries, many grains distinguish themselves by faceted boundary planes, such as (111) and (100) atomic planes. We show a typical grain of ~2 nm in diameter imaged along the [110] zone axis that is shaped by four faceted {111} and two {001} boundaries (Fig. 2A). Not all faceted boundaries are twin boundaries. Some grains are defect free, whereas others contain

[1]Shenyang National Laboratory for Materials Science, Institute of Metal Research, Chinese Academy of Sciences, Shenyang 110016, China. [2]School of Materials Science and Engineering, Shanghai Jiaotong University, Shanghai 200240, China.
*Corresponding author. Email: xyli@imr.ac.cn (X.Y.L.); lu@imr.ac.cn (K.L.)

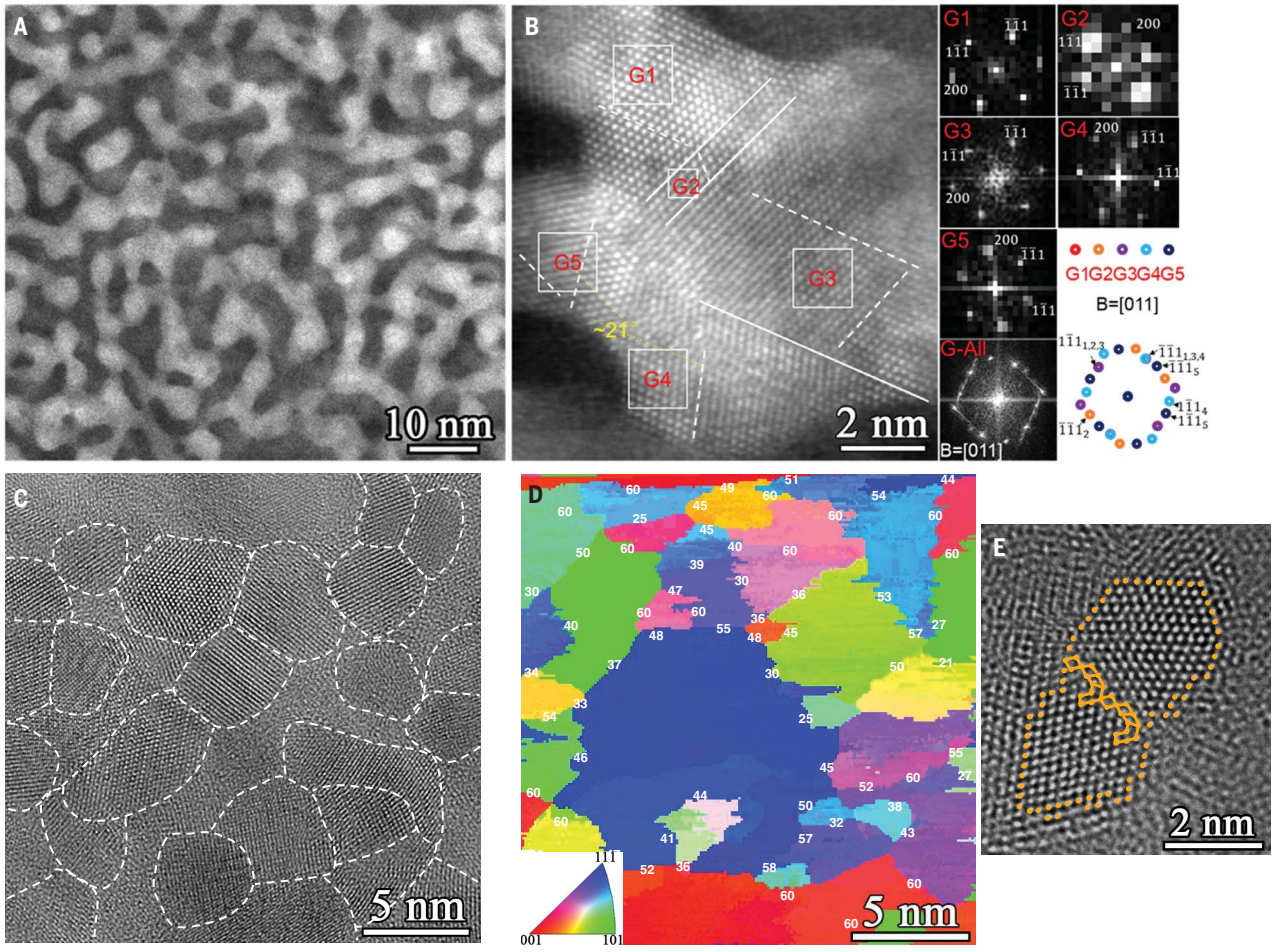

Fig. 1. Microstructures of the as-prepared Cu sample with extremely fine grains. (**A**) A typical bright-field TEM image. (**B**) (Left) A magnified image of a selected area in (A). Dashed lines represent {111} planes and solid lines show CTBs. (Right) Corresponding FFT images of grains (G1, G2, G3, G4, and G5) labeled in the left panel. G-All indicates all grains, with a schematic on the right. (**C**) A typical high-resolution TEM image. (**D**) A typical inverse pole figure (IPF) image acquired from a region in (C) from the precession electron diffraction analysis. Numbers indicate misorientation angles of GBs. (**E**) A typical structural-unit–type boundary as outlined between two tiny grains.

twins or stacking faults that cut through the grains. The twinned or faulted grains are also bounded by {111} and {001} atomic planes (Fig. 2, C and E). The {111} twin boundaries in the grains are fully coherent, with spacing of only a few atomic layers. Statistically, for grains <3 nm in size, 62% of faceted boundaries are found to be {111} and 33% are found to be {100}—a frequency ratio of about 2:1. For grains between 3 and 10 nm, the numbers are 52% {111} and 28% {100}, respectively. This feature disappears in grains >10 nm, which supports the idea that grain refining facilitates the formation of faceted {111} and {100} boundaries at the expense of other boundaries.

We also found that the shapes of those grains resemble that of the truncated octahedron (*9*). The atomic images of the defect-free grain (Fig. 2A) can be perfectly fitted with a part of a truncated octahedron projected along the [110] zone axis, except for several corners where atomic images are missing (circled in Fig. 2A). Other grains (Fig. 2, C and E) also match the twinned or faulted polyhedra very well. Lattice spots on the two corners of the grain in Fig. 2C (arrows) are blurred or absent in the TEM image. We identified a stacking fault zone between two truncated-octahedron–shaped grains (Fig. 2E), which is consistent with other observations (Fig. 1). Along the [110] projection of a truncated octahedron, four {111} and two {100} planes exist, with a frequency ratio of 2:1. This ratio is the same as what we observed in the experiments. The truncated-octahedral shape is apparently a favorable option for grains <10 nm.

We determined the thermal stability of the as-prepared Cu samples with an average grain size of 10 nm by isothermal annealing at various temperatures. We detected no apparent grain coarsening with increasing the annealing temperature up to 1348 K, which is only 9 K below the equilibrium melting point of Cu (1357 K) (Fig. 3A and fig. S3). Holding for 15 min at this temperature and cooling down, the extremely fine grains remained (Fig. 3, B and C). We still observed polyhedron-shaped grains with an average size of ~11 ± 2.3 nm with distinct boundaries—akin to what we observed before annealing. We detected more twins in the annealed grains (Fig. 3C), presumably because of the further dissociation of GBs during annealing at elevated temperatures. Elevating the temperature above 1357 K induced melting, at which point all nanograins disappeared. Our observations lead us to the conclusion that no substantial grain coarsening seems to occur before melting.

We prepared a separate sample for comparison with larger grains (average size of 25 nm) using the same process (see the supplementary materials) but with a smaller strain. We observed the onset of grain coarsening in this sample at ~985 K (Fig. 3A). The grain coarsening temperature is higher than that of 50-nm grains, which is a trend that runs contrary to the conventional belief that smaller grains coarsen at lower temperatures. Our observations support the idea that GB relaxations in polycrystals of

smaller grain size may operate more effectively to enhance the thermal stability (*6*). The Cu samples in this study are the most stable compared with the literature data for Cu (*10*–*19*), including nanograined, deformed coarse-grained, or the metastable amorphous Cu-based alloys with crystallization temperatures in the range of 0.33 to 0.36 T_m.

For the 10-nm grain–sized sample, we measured nanoindentation hardness to be as high as 4.7 ± 0.2 GPa (fig. S2). This value is equivalent to a yield strength of 1.57 GPa. This value is also higher than reported data on nanograined Cu specimens as well as amorphous Cu-based alloys (*20*–*26*). The ideal shear strength of Cu at 0 K is 2.16 GPa. The shear strength we estimated from the nanoindentation is nearly comparable to the ideal shear strength when temperature effects are considered (*27*). From previous measurements, the strength of different Cu samples follows the classical Hall-Petch relationship for grains >30 nm. For finer grains, a strength plateau or even softening occurs (*20*–*23*). By contrast, we did not find this trend in our hardness measurements. The strengthening we observed suggests that plastic deformation events, such as GB migration or sliding, must be effectively prohibited in the present Cu sample. We also found no trace of dynamic recrystallization.

The unusual stability we observed supports the belief that when grains are refined to the extreme scale, the polycrystalline structure seems to readily adopt one or more specific states. Our TEM observations, combined with the reconstructed atomic models, indicate that the truncated octahedron—either perfect or containing planar faults—is a prototype structure that represents a large portion of individual grains during the deformation-induced refinement process. Accordingly, potential structures and GB networks can be perceived on the basis of the well-known Kelvin conjecture—that is, a topological form of grains representing polycrystalline metals constructed with equal-sized grains of truncated-octahedral shape. This model provides a simple geometrical solution of idealized 3D polycrystals with nearly the minimum total area of GBs (*28*). Because a considerable fraction of GBs are Σ3-type twin boundaries in our as-prepared sample, the structure of a 3D space–filling twin boundary network must be considered as a basic precept as well (*29*).

We set up an atomistic model aimed at addressing the outstanding stability of the extremely fine Cu grains. Referring to the Kelvin model, which consists of two ideal truncated-octahedra of equal size with their centers (K1 and K2; Fig. 4A) in a body-centered cubic array, we constructed an extended Kelvin supercell with 16 truncated-octahedral–shaped grains of equal size. We can recognize

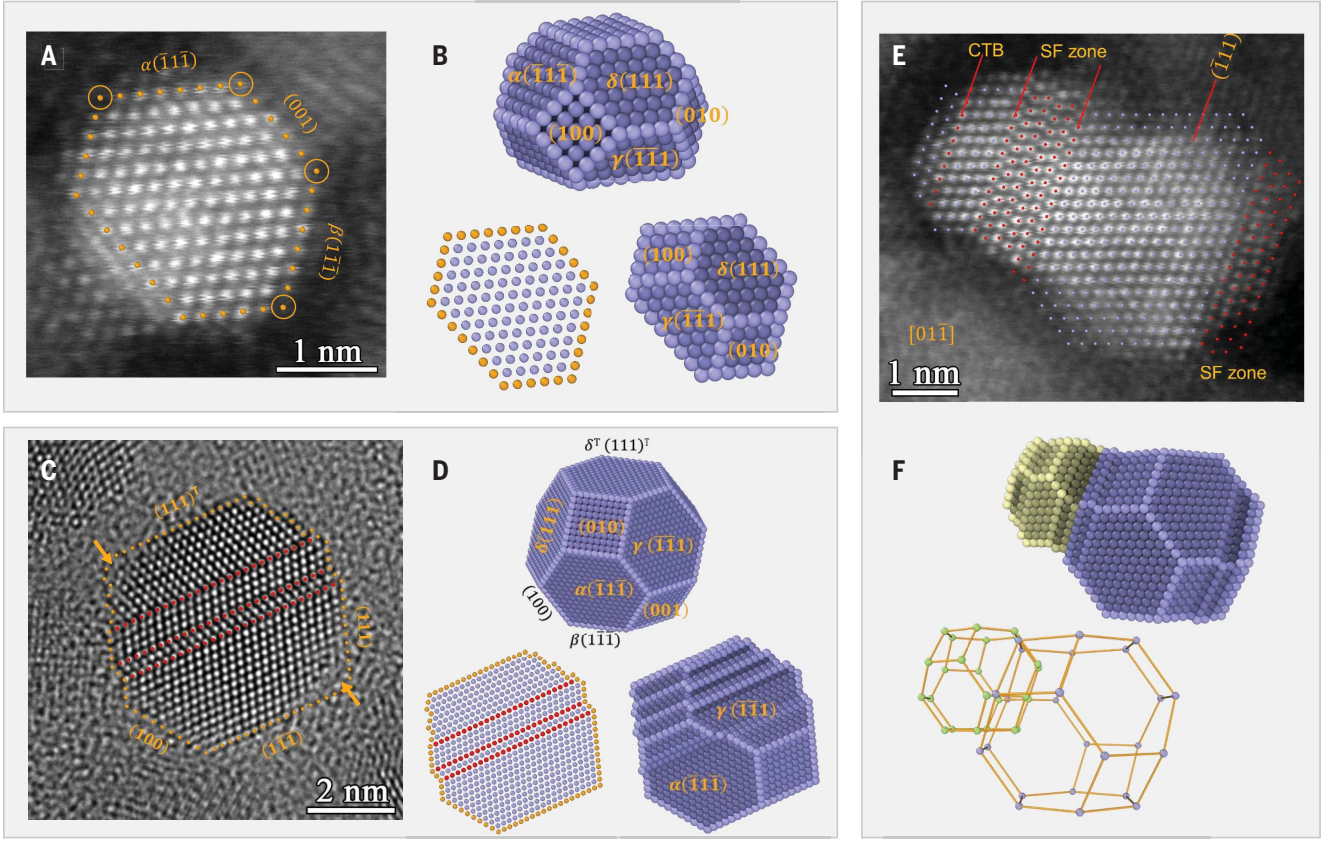

Fig. 2. High-resolution TEM images of individual grains with truncated-octahedral geometries. (**A**) A tiny grain of ~2 nm in size. (**B**) A part of an ideal truncated-octahedron with 1154 atoms (top), rotated by 49° along the [110] axis (lower right). The projected atomic positions on the (001) plane (lower left) are coincident with the TEM image in (A) (where only border atoms are shown in orange). Corner atoms in blurred contrast are circled in (A). (**C**) A grain containing twins. (**D**) An ideal truncated-octahedron of 11,817 atoms (top), rotated by 25.5° about the [01$\bar{1}$] axis after introducing twins (lower right). Projected atomic positions (bottom left) agree with the TEM image in (C) (where only border atoms in orange and twin boundary atoms in red are shown). Missing corners are indicated by orange arrows in (C). (**E**) Two grains containing stacking faults (SFs) and twins. (**F**) Two attached truncated-octahedral grains of different sizes with projected atomic positions agreeing with the TEM image in (E).

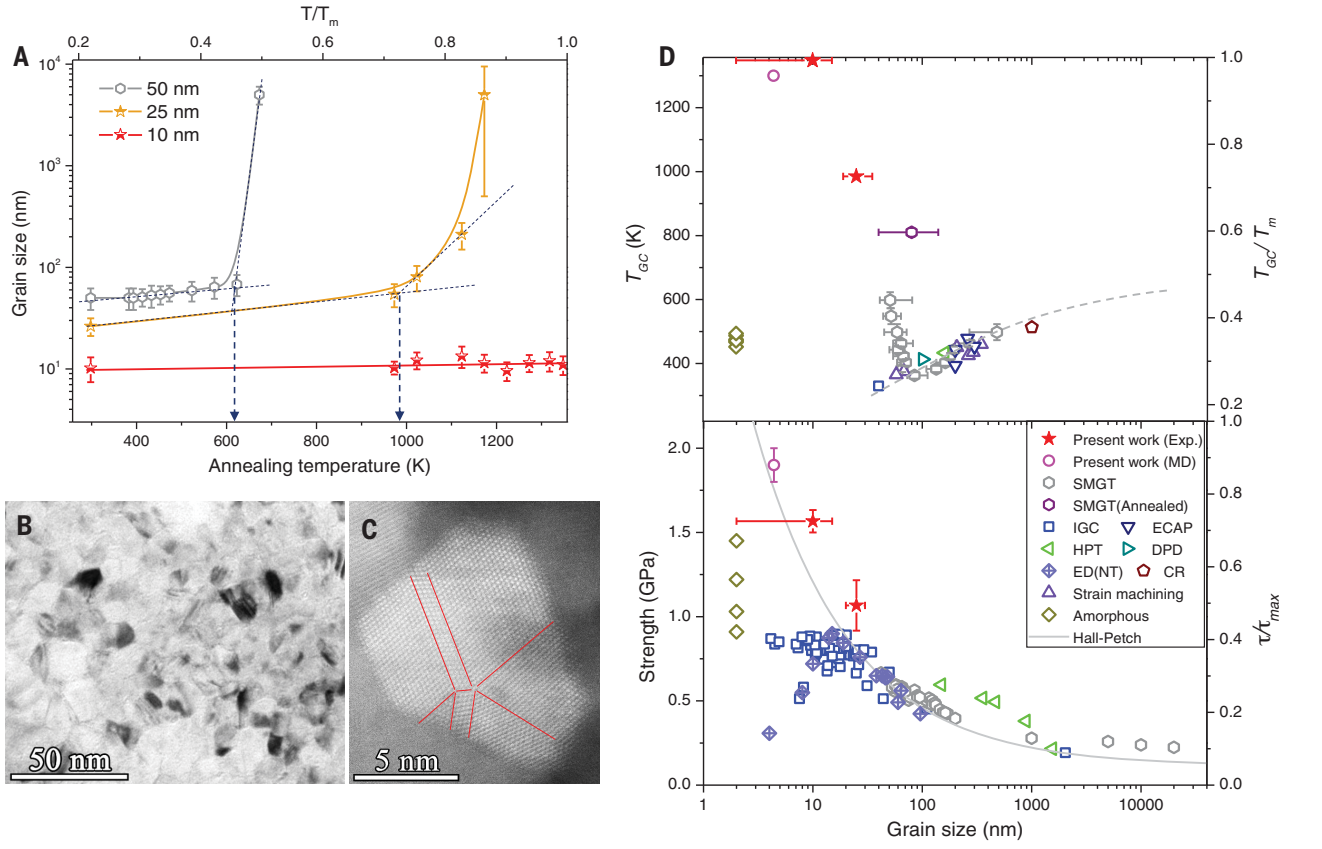

Fig. 3. Extremely high thermal stability and strength. (**A**) Grain size variations as a function of annealing temperature for three samples with initial average grain sizes of 50 nm, 25 nm, and 10 nm, respectively. Each point of grain size was averaged from >300 grains. (**B**) A TEM image of the sample with an initial grain size of 10 nm after annealing at 1348 K for 15 min. (**C**) A high-resolution TEM image of a grain in (B). Red lines indicate twin boundaries. (**D**) Grain coarsening temperatures (T_{GC}) and strength as a function of grain size in pure Cu. Literature data for Cu samples prepared through various processes in (*6*, *10*–*17*, *20*–*24*) are included. Data for amorphous Cu alloys are from (*18*, *19*, *25*, *26*). T_m, melting point of Cu; τ_{max}, ideal shear strength of Cu (*27*). Each grain coarsening temperature was obtained from three independent experiments, and each strength datum was obtained from 10 independent experiments. Exp., experimental; SMGT, surface mechanical grinding treatment; IGC, inert gas condensation; ECAP, equal channel angular pressing; HPT, high-pressure torsion; DPD, dynamic plastic deformation; ED(NT), electrodeposition (nanotwin); CR, cold rolling.

the fundamental characteristics of GBs, and twin boundary networks can be recognized. By taking polyhedron O1 as the center cell, we can specify the lattice orientation of its eight nearest neighboring grains such that each {111} face of O1 can form a Σ3 coherent twin boundary (CTB) with them—i.e., A1, B1, C1, D1 (upper) and A2, B2, C2, D2 (lower). The lattice orientations of the six second-nearest neighboring grains to O1 (I1, E1, F1 and I2, E2, F2) are not strongly limited. We chose them such that in each <001> orientation, a Σ9-type tilt GB is formed with O1 (or O2) (fig. S4 and table S2). Our result confirms the theoretical prediction (*29*) that a 3D space–filling CTB network can be constructed by a specific arrangement of truncated octahedra in fcc solids.

By choosing an extended Kelvin polycrystal with an initial grain size of 3.27 nm as a starting structure for simplicity, we carried out MD simulations to relax the sample by heating it up to different target temperatures at a rate of 8 K/ns. We based the interatomic potential on the semiempirical model developed with the embedded atom methods (EAM) (*30*). For comparison, we also conducted MD tests on a number of samples representing cases for flat and curved GBs, in which both grain size and orientations are treated as free variables (fig. S6).

During MD relaxation and subsequent heating, GBs in the extended Kelvin polycrystal transform into different structures through extensively GB reaction and migration events. With increasing temperature, GB reactions—such as dissociation and coalescence of GBs associated with some Σ9-type GBs—are triggered at triple lines or junctions of GBs, as expected experimentally (*31*) and theoretically (*29*). Migration of twist GBs becomes substantial at mediate temperatures (640 K), and it is close to that for curved GBs observed in separate simulations (fig. S6). The preexisting CTB network is stable against thermal fluctuations. After heating to 760 K, although some grains shrank and finally disappeared because of GB migration, the entire GB network failed to collapse. The GBs merged and developed into a different form that topologically resembles the Schwarz D-surface (*32*, *33*). As a triply periodic minimal surface, we can identify the shape of the Schwarz D-interface in our calculations (Fig. 4B and fig. S5).

This transformation is thermodynamically driven by minimizing the interface area, as indicated by the MD results. Although the Kelvin polycrystal provides a reasonable solution for an efficient, space-filling arrangement of grains, the total boundary area was further minimized by forming the Schwarz D-interface structure (*34*). Our observation indicates that the polycrystalline structure with Schwarz D-interfaces is more stable than the Kelvin polycrystals, but this does not necessarily mean that such a transformation occurs at a distinct point during the refinement of coarse grains into the nanograins. Our MD simulations also confirmed that the Schwarz D-structure can be obtained by imposing strain at low temperatures. The

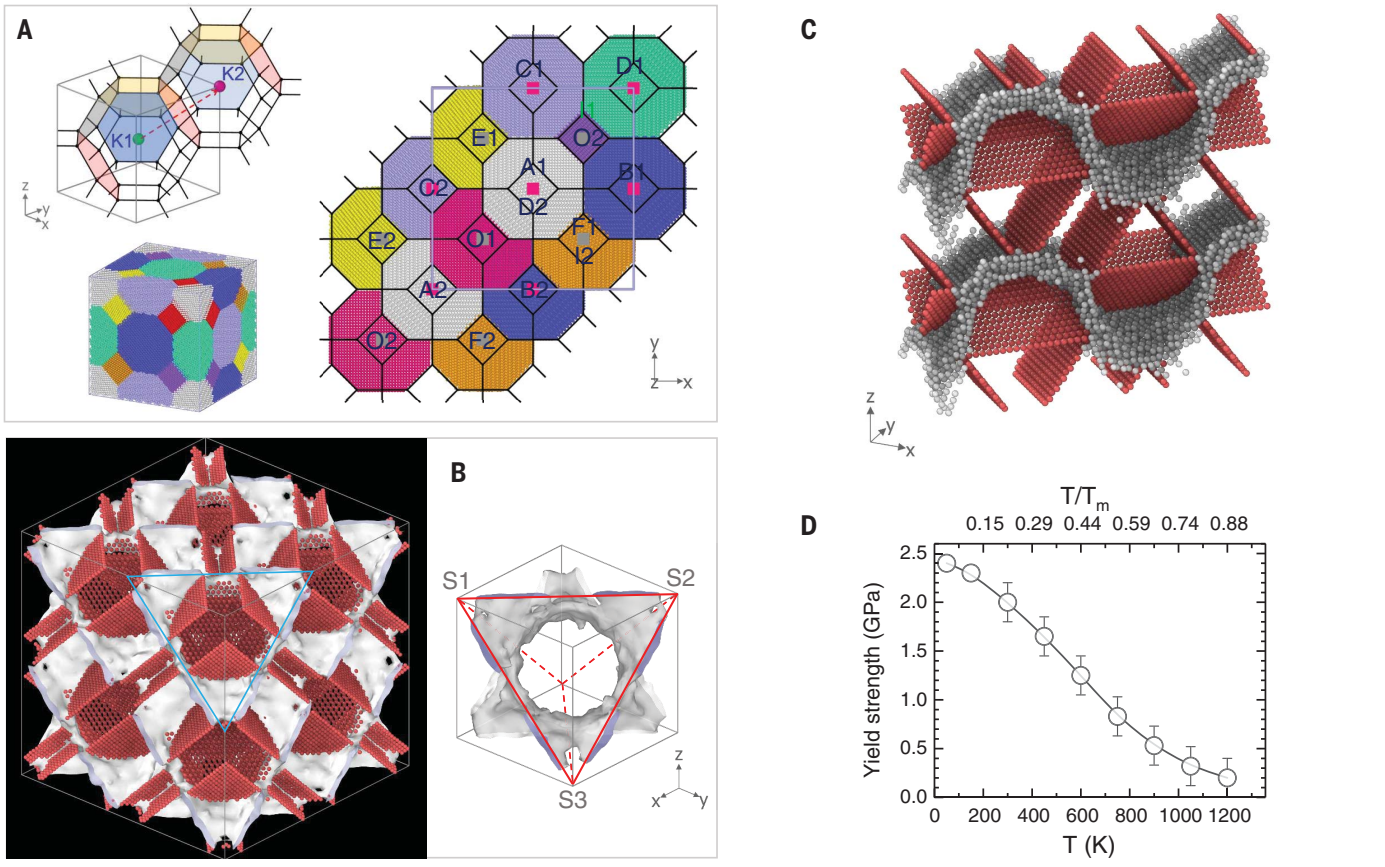

Fig. 4. Atomistic model and MD simulations of Schwarz crystals. (**A**) The original Kelvin model of two ideal truncated-octahedra of equal volume (K1 and K2) in 1 by 1 packing (top left). A polycrystal of 16 grains (right) was constructed using a 4 by 4 packing Kelvin model (initial grain size, 6.6 nm). A space-filling 3D CTB network was constructed with a specified lattice orientation for individual grains (see Supplementary Materials). (**B**) (Left) MD-obtained twin-bounded polycrystalline structure at 0 K, demonstrated by 2 by 2 by 2 supercells where atoms in fcc lattice sites are removed. (Right) GBs resembling the Schwarz D-interface in a 1 by 1 by 1 supercell. (**C**) A section-view of the Schwarz crystal showing Schwarz D-GBs constrained by CTB networks. (**D**) The MD-obtained yield stress as a function of temperature. Error bars quantify uncertainty caused by rate effects and thermal fluctuations.

adoption of the minimal-interface structure constitutes an energetically more-favorable GB relaxation process under thermal and mechanical stimuli.

The Schwarz D-interface is constrained by high-density CTBs on both sides (Fig. 4C)—a structure meant to suppress GB migration. With the minimal-interface area and the zero-mean curvature (another characteristic of minimal interface structures), the driving force to migrate the GBs tends to vanish, which is proportional to the GB curvature. CTBs are intrinsically stable at elevated temperatures. The stable CTB networks and Schwarz D-interface interlock with each other, preventing GBs from developing substantial curvatures to escape and CTBs from migrating. Such a pronounced stability cannot be achieved with the Schwarz D-interface only, nor with only the nanotwinned structures.

The obtained Schwarz D-structure stays stable at elevated temperatures. Rather than grain coarsening, roughening of GBs occurs as the melting point is approached, at which point the liquid phase is nucleated heterogeneously at 1321 K (fig. S6). This suggests that the upper thermal stability is limited kinetically by GB melting. This notable stability agrees fully with our experimental results (Fig. 3). Clearly, preventing the migration of GBs through a minimal interface constrained by a 3D CTB network constitutes the key mechanism to achieve the pronounced stability for polycrystals at such extreme sizes.

We conducted uniaxial tensile-loading tests on the CTB-constrained Schwarz D-structure at various temperatures and strain rates (10^5 to 10^7 s^{-1}) (fig. S7). GB activities such as sliding or migration can be suppressed entirely. The primary mode of deformation is twinning. For example, a twinning partial dislocation is generated from one GB site and absorbed at the opposite GB, which results in migration of the twin boundary plane. Generating a stacking fault to a glide plane parallel to the CTB is also possible during the plastic deformation. The critical stress corresponding to incipient twinning is temperature-dependent (Fig. 4D). The yield strength is 1.8 to 2 GPa at 300 K, which is higher than our experimentally measured data, possibly owing to the grain size distribution in real samples. The strength at 10 K is comparable to the ideal pure shear strength obtained through first-principle calculations (*27*).

Evidence based on our experiments and MD simulations confirms that a pronounced stability is achievable if the minimal-interface structure constrained by a CTB network is adopted in polycrystalline Cu with nanosized grains. The structure, which we refer to as a Schwarz crystal, is a different kind of metastable state for polycrystalline solids. This state differs fundamentally from the amorphous solid states. Because the metastable structure is formed when twinning—either thermally induced or deformation induced—and is effective in relaxing GB structures, the appearance of the Schwarz crystal in different metals and alloys is expected with the activation of twinning mechanisms at

the nanoscale. The pure Cu Schwarz crystal, which contains a very high density of interfaces, exhibits a thermal stability as high as that of a single crystal and much higher than that of amorphous solids. Therefore, the structure provides emerging opportunities for exploring physical and chemical phenomena of metals, particularly with respect to transport dynamics of atoms and electrons at interfaces and interactions of various defects at high temperatures. As a benchmark structure capable of suppressing grain coarsening under both thermal fluctuations and external forces, the Schwarz crystal allows for elevated stability and strength that goes with refining grains into the extremely fine scale. This overcomes some of the difficulties present in traditional strategies for materials development. In principle, the Schwarz crystal should be accessible in other materials and may provide a different direction for developing strong and stable materials for high-temperature applications.

REFERENCES AND NOTES

1. R. Zallen, *The Physics of Amorphous Solids* (Wiley, 1983).
2. P. Haasen, B. L. Mordike, *Physical Metallurgy* (Cambridge Univ. Press, 1996.)
3. K. Lu, *Nat. Rev. Mater.* **1**, 16019 (2016).
4. P. Färber, E. Cadel, A. Menand, G. Schmitz, R. Kirchheim, *Acta Mater.* **48**, 789–796 (2000).
5. C. A. Schuh, T. G. Nieh, H. Iwasaki, *Acta Mater.* **51**, 431–443 (2003).
6. X. Zhou, X. Y. Li, K. Lu, *Science* **360**, 526–530 (2018).
7. X. Zhou, X. Y. Li, K. Lu, *Phys. Rev. Lett.* **122**, 126101 (2019).
8. W. Longley, T. J. McIntosh, *Nature* **303**, 612–614 (1983).
9. C. Chieh, *Acta Cryst.* **A35**, 946–952 (1979).
10. C. Saldana, A. H. King, S. Chandrasekar, *Acta Mater.* **60**, 4107–4116 (2012).
11. X. Y. Li, X. Zhou, K. Lu, *Sci. Adv.* **6**, eaaz8003 (2020).
12. A. Kumpmann, B. Günther, H. D. Kunze, *Mater. Sci. Eng. A* **168**, 165–169 (1993).
13. N. Lugo, N. Llorca, J. J. Suñol, J. M. Cabrera, *J. Mater. Sci.* **45**, 2264–2273 (2010).
14. C. F. Gu, C. H. J. Davies, *Mater. Sci. Eng. A* **527**, 1791–1799 (2010).
15. Y. Zhang, N. R. Tao, K. Lu, *Acta Mater.* **56**, 2429–2440 (2008).
16. P. Jenei, J. Gubicza, E. Y. Yoon, H. S. Kim, J. L. Lábár, *Compos. A: Appl. Sci. Manuf.* **51**, 71–79 (2013).
17. Z. N. Mao *et al*., *Mater. Sci. Eng. A* **674**, 186–192 (2016).
18. B. W. Zhang, X. L. Shu, S. Y. Zhu, S. Z. Liao, *J. Mater. Proc. Tech.* **91**, 90–94 (1999).
19. H. Zhang, Z. Tan, B. Zhang, X. Shu, J. Yu, *J. Mater. Sci. Lett.* **10**, 45–46 (1991).
20. L. Lu, X. Chen, X. Huang, K. Lu, *Science* **323**, 607–610 (2009).
21. A. H. Chokshi, A. Rosen, J. Karch, H. Gleiter, *Scr. Metall.* **23**, 1679–1683 (1989).
22. G. E. Fougere, J. R. Weertman, R. W. Siegel, *Nanostruct. Mater.* **3**, 379–384 (1993).
23. P. G. Sanders, J. A. Eastman, J. R. Weertman, *Acta Mater.* **45**, 4019–4025 (1997).
24. H. G. Jiang, Y. T. Zhu, D. P. Butt, I. V. Alexandrov, T. C. Lowe, *Mater. Sci. Eng. A* **290**, 128–138 (2000).
25. W. H. Wang, *J. Appl. Phys.* **99**, 093506 (2006).
26. Y. P. Deng *et al*., *Intermetallics* **15**, 1208–1216 (2007).
27. S. Ogata, J. Li, S. Yip, *Science* **298**, 807–811 (2002).
28. F. N. Rhines, K. R. Craig, R. T. DeHoff, *Metall. Trans.* **5**, 413–425 (1974).
29. V. Y. Gertsman, B. W. Reed, *Z. Metallk.* **96**, 1106–1111 (2005).
30. V. Borovikov, M. I. Mendelev, A. H. King, R. LeSar, *Model. Simul. Mater. Sci. Eng.* **23**, 055003 (2015).
31. T. Yu, N. Hansen, X. Huang, *Proc. R. Soc. A.* **467**, 3039–3065 (2011).
32. H. A. Schwarz, *Gesammelte Mathematische Abhandlungen*, vols. 1 and 2 (Springer, 1890).
33. A. L. Mackay, *Nature* **314**, 604–606 (1985).
34. L. E. Scriven, *Nature* **263**, 123–125 (1976).

ACKNOWLEDGMENTS

We thank C. Y. Wu for help with sample preparation. **Funding:** This work is funded by the Ministry of Science and Technology of China (grant nos. 2017YFA0204401 and 2017YFA0700700) and the Chinese Academy of Sciences. **Author contributions:** X.Y.L. and K.L. developed the concept, designed the experiments, and supervised the projects. X.Z. and X.Y.L. prepared the samples and characterized structures. X.Z. measured properties. Z.H.J. performed modeling and simulations. All authors discussed and analyzed the results. X.Y.L., Z.H.J., and K.L. wrote the paper. **Competing interests:** The authors declare no competing interests. **Data and materials availability:** All data are available in the manuscript or the supplementary materials.

SUPPLEMENTARY MATERIALS

science.sciencemag.org/content/370/6518/831/suppl/DC1
Materials and Methods
Supplementary Text
Figs. S1 to S7
Tables S1 to S3
References (*35*–*44*)

1 August 2020; accepted 8 October 2020
10.1126/science.abe1267

Constrained minimal-interface structures in polycrystalline copper with extremely fine grains

X. Y. Li, Z. H. Jin, X. Zhou and K. Lu

Science **370** (6518), 831-836.
DOI: 10.1126/science.abe1267

Locking in nanoscale strength

Metals with nanometer-sized crystal grains are super strong, but they do not generally retain their structure at higher temperatures. This property undermines their high strength and makes their use in applications challenging. Li *et al.* found a minimum-interface structure in copper with 10-nanometer-sized grains that, when combined with a nanograin crystallographic twinning network, retains high strength to temperatures just below the melting point. This discovery suggests a different path forward for stabilizing nanograined metals.

Science, this issue p. 831